Computational Materials Science 46 (2009) 239–244

Contents lists available at ScienceDirect

Computational Materials Science

journal homepage: www.elsevier.com/locate/commatsci

Structures and structural evolution of Pt_n (n = 15–24) clusters with combined density functional and genetic algorithm methods

Xianglei Wang [a], Dongxu Tian [a,b,*]

[a] State Key Laboratory of Fine Chemicals, School of Chemical Engineering, Dalian University of Technology, 158 Zhongshan Road, Dalian 116012, China
[b] College of Advanced Science and Technology, Dalian University of Technology, Dalian 116024, China

ARTICLE INFO

Article history:
Received 15 October 2008
Received in revised form 15 February 2009
Accepted 24 February 2009
Available online 14 April 2009

PACS:
31.15.Ew
61.46.+w
71.15.−m
73.22.−f

Keywords:
Metals
Nanostructures
Electronic states

ABSTRACT

Low-lying structures and structural evolution of Pt_n (n = 15–24) clusters were studied using a genetic algorithm followed by local optimization with density functional theory calculations. As a whole, the lowest energy structures of Pt_n (n = 15–24) clusters are likely to form open structural motifs not the atomic closed shell structures. Four kinds of structural motifs, i.e., dodecahedron based (DODB), cuboctahedron based (COB), layered triangular (LT) and cubic configurations have been investigated for the medium-sized Pt_n (n = 15–24) clusters. The Pt_n (n = 15–16, 19, 24) prefer the DODB growth pattern. While the Pt_n (n = 17–18, 20) lean to the LT configuration. The lowest energy structures of Pt_{21} and Pt_{23} clusters adopt the cubic structure. Pt_n clusters at n = 15, 18, 24 are relatively more stable and these clusters are "magic" numbered. Three different spin multiplicities (M = 1, 3 and 5) have been examined for Pt_n (n = 15–24) clusters, and found that the most stable Pt_{22} cluster is the only one in triplet state. These results are significantly different from those predicted in earlier works. The relationship between electronic property and geometry was also discussed.

© 2009 Published by Elsevier B.V.

1. Introduction

The chemical and physical properties of metal clusters have attracted much attention in recent years [1], both for the interest presented by their specific properties and as models of surfaces and crystals. Platinum clusters are of particular significance because they offer a wide range of interesting properties as well as a variety of technology applications. Due to their unique properties, platinum clusters are widely used as catalysts [2], Pt cluster also plays an important role in the development of the hydrogen-based fuel economy, particularly in the proton exchange membrane-type hydrogen fuel cell [3].

Experimental determination of the ground state structure for small platinum clusters is difficult. So there are only a small minority of studies using a wide range of spectroscopic techniques, viz., laser induced fluorescence, resonance two-photon ionization and dissociation methods, stark spectra [4–10]. Theoretical studies using the first-principles [11–25] and empirical potentials methods [26–31] have been reported. The most stable structures of small platinum clusters are still an issue in debate. Bhattacharyya and Majumder [19], Kumar's group [25] have reported that up to n = 9, Pt_n clusters favor planar geometries and a structural transition to non-planar geometries occur at n = 10. While the other results [13,21,28] reported that the most stable structures of Pt_n clusters from n = 4 usually adopt 3D configurations based on tetrahedron, octahedron, square pyramid and pentagonal bipyramid geometries. For medium-sized clusters, Kumar and Kawazoe reported that layered and pyramid-based structures are favorable in the range of Pt_n (n = 10–20), the simple cubic structures are favorable up to 38, and octahedral motifs are favorable for n > 38 [25]. For larger platinum clusters, the lowest-energy isomers adopt the three of the morphologies: icosahedral, decahedral and truncated octahedral obtained by using the empirical potentials methods [27–29]. In addition, Pt_{13} and Pt_{55} clusters are the main focus of attention. For Pt_{13}, a cuboctahedron was found [16] to be lower in energy than an icosahedron isomer. However, a low symmetry disordered structure [14] and a buckled biplanar layered structure [11] were reported to be more stable than the two former structures. A peculiar structural rearrangement was found for Pt_{55} cluster [15] based on cuboctahedron which had been reported [20] as the most stable isomer. All these findings indicate that the structural growth sequence of Pt_n clusters is rather complicated and requires very careful examinations.

* Corresponding author. Address: State Key Laboratory of Fine Chemicals, School of Chemical Engineering, Dalian University of Technology, 158 Zhongshan Road, Dalian 116012, China.
E-mail address: tiandx@dlut.edu.cn (D. Tian).

0927-0256/$ - see front matter © 2009 Published by Elsevier B.V.
doi:10.1016/j.commatsci.2009.02.031

Table 1
Bond length (r), binding energy (E_b), vibration frequency (ω), and vertical ionization potential (VIP) of Pt_2 dimer from our DFT calculations at PBE/DNP/DSPP level compared with experimental results.

	r (Å)	E_b (eV)	ω (cm^{-1})	VIP (eV)
Expt.	2.34 [6]	3.14 ± 0.02 [7]	217.2 [7]	8.68 ± 0.02 [8]
This work	2.39	3.59	215.6	8.91

Within the medium sized range of n = 15–24, less attention has been paid to Pt_n clusters. Here we performed a comprehensive search using a combination of empirical potentials and first-principles method to elucidate the size-dependent structure evolution of medium-sized Pt_n (n = 15–24) clusters and to determine the most stable structure for each size. The semiempirical potential may miss some structures (like cage structures), thus we also considered some special cage motifs to ensure the completeness of structure search for the intermediate Pt clusters. Instead of the generally believed icosahedron-based and decahedron-based structures, our extensive search revealed that the DODB, LT and cubic structures dominate the growth sequence of Pt_n (n = 15–24) clusters. In particular, Pt_{15} with octahedral structure shows an extraordinary sta-

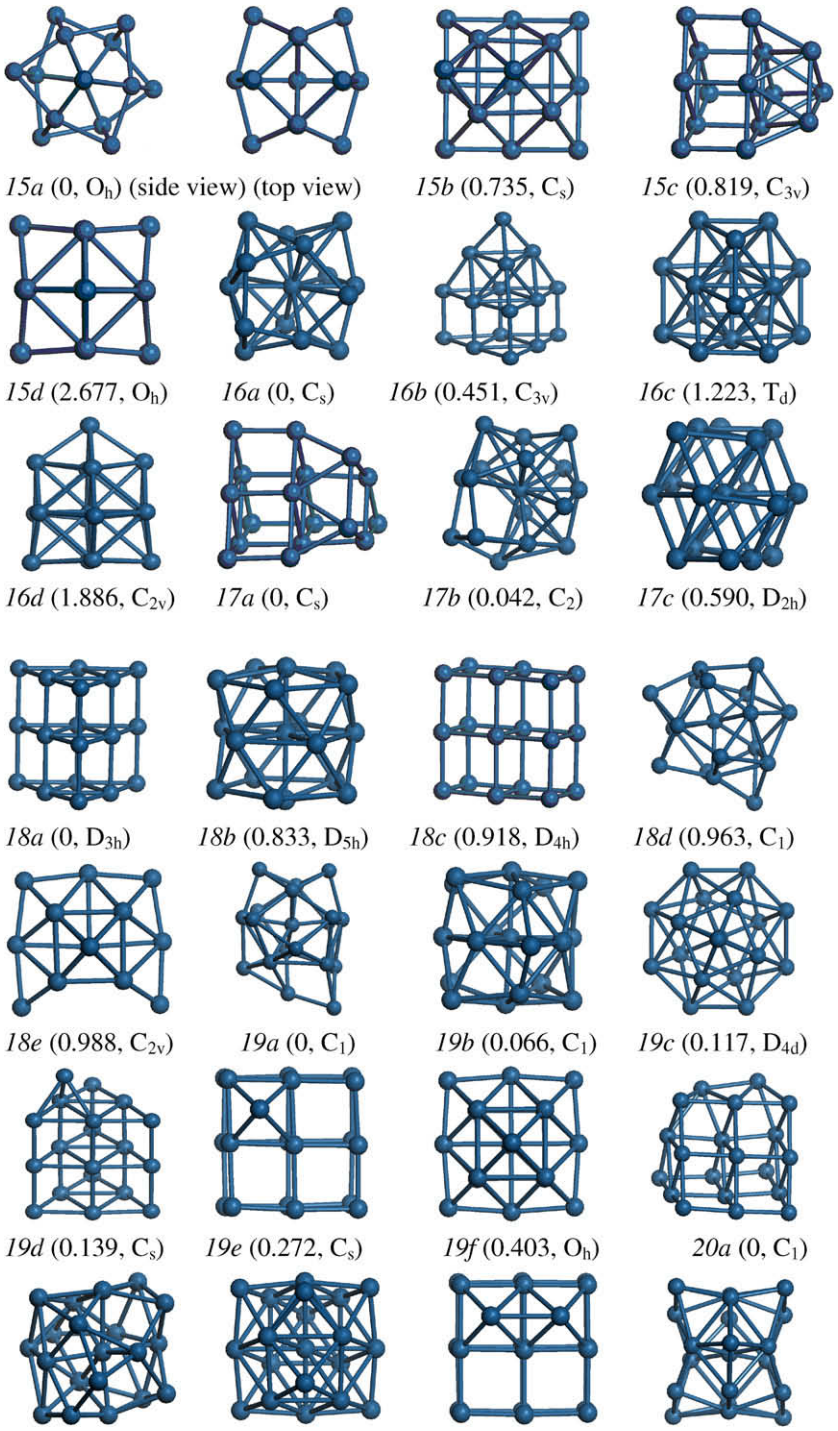

Fig. 1. Low-lying isomers of Pt_n clusters(n = 15–24). The number in brackets refers to the energy (eV) relative to the lowest-energy isomer, symmetry is followed.

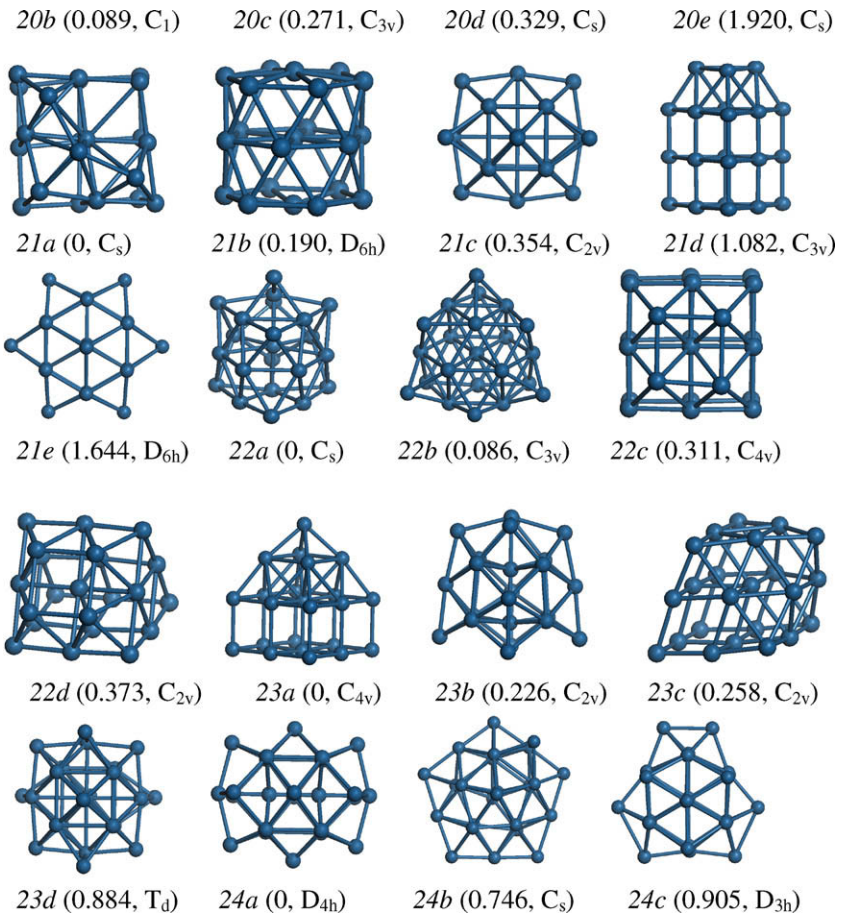

Fig. 1 (*continued*)

bility and is named a "magic" size. The influence of multiplicities (M = 1, 3 and 5) on the stability of isomers were studied. In addition, the relationship between electronic property and cluster geometry was discussed.

2. Methodological details

In order to search the lowest energy structures of platinum clusters, we used the extensive empirical genetic algorithm and DFT method to explore the potential energy surface (PES) of the clusters. The initial structures were partly generated by genetic algorithm [32] (GA). The interatomic interaction is approximated by six types of many-body potential such as Gupta-like [33–35] and Sutton–Chen potentials [36], etc. The GA was shown to be an effective way to produce a large number of isomers for further DFT optimization [37]. At each size, 32–64 arbitrary configurations were generated as the initial population. Two configurations from the population were chosen randomly as parents to produce an offspring through mating and mutation operations. The offspring cluster was then fully relaxed using molecular dynamics [33–36]. If the energy of the offspring was lower than that of one of the parents, the offspring would replace the parent with the higher energy. This procedure was repeated until the lowest energy structure in the population remained unchanged in 5000 consecutive iterations. The semiempirical potential may miss some important motifs. In the present work, some growth pattern isomers, for example, layered triangular and caged motifs are also considered. In addition, previously reported important structures were also taken into account. At each cluster size, about 70–120 isomers were considered.

Then these structures were fully relaxed at the DFT level without symmetry constrains. We adopted the PBE exchange-correlation functional [38] within the generalized gradient approximation (GGA) as well as a DFT-based relativistic semi-core pseudopotential (DSPP) [39], and a double numerical basis set including d-polarization functions (DNPs), as implemented in DMol package [40]. Spin unrestricted calculations have always been performed. The accuracy of the present PBE/DNP/DSPP scheme was checked on platinum dimer. The theoretical results of bond length, binding energy, vibration frequency, and vertical ionization potential for Pt_2 agree with experimental ones [6–8] satisfactorily as shown in Table 1.

3. Results and discussion

3.1. Structural evolutions of low-lying isomers for Pt_n (n = 15–24) clusters

A large amount of low-lying isomers obtained here can be sorted into four kinds of structural motifs: bent rhombic dodecahedron based (DODB), cuboctahedron based (COB), layered triangular (LT) and cubic. To simplify, we selected the most stable configuration in each motif as representative at each cluster size. The low-lying representative isomers and their symmetries, energies differences for Pt_n (n = 15–24) clusters are shown in Fig. 1. The tolerance in bond length for cluster symmetry is 0.1 Å. We assign labels to each cluster isomers such as "*15a*", where the first number is the number of atoms in the cluster and the letter gives the rank of isomers in the order of increasing energy (*Xa* means the lowest-energy isomer). The size-dependent binding energies for these

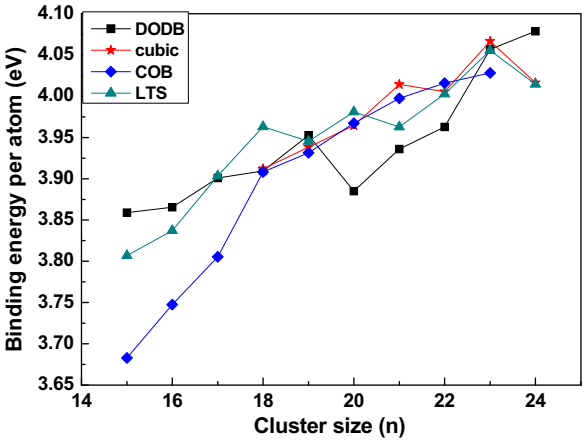

Fig. 2. Binding energy per atom as a function of Pt_n (n = 15–24) for four different growth pattern isomers. Color and symbolic code: DODB (black, square), cubic (red, star), COB (blue, diamond) and LTS (olive, upper triangle).

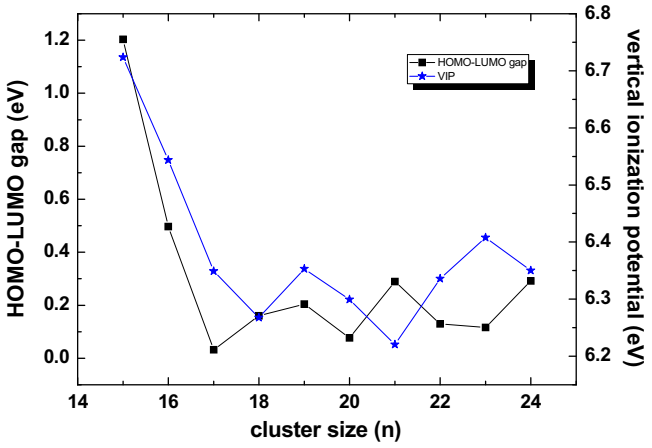

Fig. 3. The abscissa axis is the number of atoms for Pt_n (n = 15–24) clusters. For the right vertical axis, the black solid line with squares gives the value of the HOMO–LUMO gap; for the left vertical axis, the blue solid line with star gives the value of vertical ionization potential.

structural motifs are compared in Fig. 2. Binding energy per atom, mean coordination number and d electron bandwidth for the lowest energy structures are listed in Table 2.

3.1.1. Pt_n (n = 15–16, 19, 24) clusters

A bent rhombic dodecahedron (*15a*, shown in Fig. 1) is staring with a central atom surrounded by an octahedron of six first-neighbors (Pt_7), then adding eight second-neighbors capped on eight faces of the octahedron. This isomer (*15a*) has the highest binding energy. As a continuation of Pt_{15}, bent rhombic dodecahedron based (DODB) configurations dominates the growth pattern for Pt_n (n = 16, 19, 24) clusters. Relative to other kinds of structures, the DODB configuration lies lower in energy by at least 0.735, 0.451, 0.905 eV than the other kind of isomers for Pt_{15}, Pt_{16} and Pt_{24}, respectively. As shown in Fig. 2, the most stable isomer (*16a*) for Pt_{16} adopts the skeleton of *15a*, with one embedded atom squeezing into one rhombus, and sequentially the original quadrilateral is replaced by one pentatomic ring. The lowest energy structure for Pt_{19} is an amorphous structure obtained by adding four atoms on the asymmetry sites of isomer (*15a*). The most stable structure for Pt_{24} can be seen as a conjoined twin structure of two bent rhombic dodecahedrons. At Pt_{15}, a capped square pyramid (*15b*), a LT isomer (*15c*, the most stable isomer reported by Kumar and Kawazoe) and a distorted COB configuration (*15d*) lie 0.735, 0.819 and 2.677 eV higher in energy than (*15a*), respectively. A double hexagonal bipyramid structure whose two hexagonal planes are rotated with respect to each other like the rotated pentagonal rings in the 13-atom icosahedron was argued to be the lowest energy structure by previous calculations with empirical potential [28]. However, it lies 3.888 eV higher in energy than the present isomer (*15a*). At Pt_{16}, a LT isomer (*16b*, the most stable structure in Ref. [25]), a truncated tetrahedron (*16c*) and a distorted COB isomer (*16d*) lie 0.451, 1.223 and 1.886 eV higher in energy than (*16a*), respectively. In addition, cage structures and structures obtained from empirical potentials [27,28] are also considered. But they lie at least 0.543 eV higher in energy than (*16a*). For Pt_{19}, a double icosahedron was viewed as the lowest energy structure by empirical potential method [28], and an octahedron with closed atomic shell was considered to be the most stable isomer using first-principles calculations (*19f*) [20]. But they lie 3.930 and 0.403 eV higher in energy than the present result (*19a*), respectively. The second low-lying isomer (*19b*) obtained from (*18b*) and the layer stacking structure (*19c*) with D_{4d} symmetry are only 0.066 and 0.117 eV higher in energy than (*19a*), respectively. Isomers (*19d* and *19e*) with one atom capped on (*18a*) and (*18c*) lie 0.139 and 0.272 eV higher in energy, respectively. For Pt_{24}, a decahedron-based isomer (*24b*) which is regarded as the most stable structure by Kumar and Kawazoe [25] is 0.746 eV higher in energy than the present (*24a*). D_{3h} symmetry (*24c*), layered triangular and cubic isomers lie 0.905, 1.530 and 1.490 eV higher in energy at n = 24, respectively.

3.1.2. Pt_n (n = 17–18, 20) clusters

The layered triangular growth pattern are favorable for Pt_n (n = 17–18, 20) clusters. This is in agreement with the results reported by Kumar and Kawazoe [25]. As shown in Fig. 1, (*18a*) is a trilayered triangular prism with closed atomic shell. (*17a*) can be obtained from (*18a*) by removing a center atom of one edge, and (*20a*) by adding two atoms on a square face of (*18a*). For Pt_{17}, a dodecahedron based configuration (*17b*) and a COB (*17c*) isomer are 0.042 and 0.590 eV higher in energy than (*17a*). The icosahedron-based isomer [27] and hexagonal bipyramid based isomer [28] are significantly higher in energy than (*17a*). The values are 0.945 and 0.376 eV, respectively. At Pt_{18}, a five-fold trilayer (*18b*), a four-cube isomer (*18c*), a DODB structure (*18d*) and a COB isomer (*18e*) are 0.833, 0.918, 0.963 and 0.988 eV higher in energy than (*18a*), respectively. The isomers obtained by empirical potentials [27,28] lie higher by at least 1.8 eV in energy than the present (*18a*). For Pt_{20} cluster, (*20b*) obtained from (*18b*) by adding two atoms in the top and middle plane lies only 0.089 eV higher in energy. A COB isomer (*20c*), a cubic isomer (*20d*) and a DODB isomer

Table 2
Binding energy (E_b) per atom, ACN and d-bandwidth for Pt_n (n = 15–24) clusters.

		Pt_{15}	Pt_{16}	Pt_{17}	Pt_{18}	Pt_{19}	Pt_{20}	Pt_{21}	Pt_{22}	Pt_{23}	Pt_{24}
E_b (eV)		3.86	3.87	3.9	3.96	3.95	3.98	4.01	4.02	4.07	4.08
ACN	Lowest energy structures	5.07	4.75	4.35	4.33	4.95	4.70	4.38	5.55	4.96	5.42
	Closed packing structures	6.67	6.0	6.82	5.78	7.16	6.0	5.90	5.91	6.70	6.25
d-Bandwidth (eV)		7.0	6.82	5.84	5.92	6.73	6.27	6.67	6.63	6.73	6.87

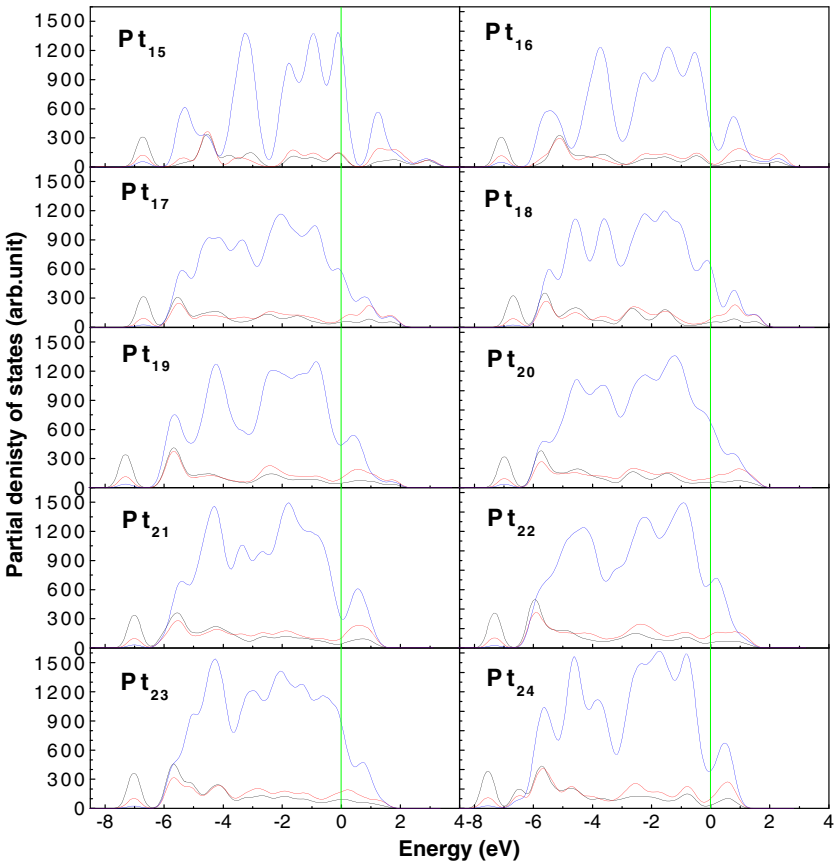

Fig. 4. PDOS for the lowest-energy Pt_n (n = 15–24) clusters. Fermi energy is set as zero on the energy axis with the green line. Black: s states; red: p states; blue: d states.

(*20e*) are 0.271, 0.329 and 1.920 eV higher in energy than (*20a*), respectively. The energy difference between (*20a*) and a capped double icosahedron obtained from empirical methods [28] is 1.973 eV higher in energy.

3.1.3. Pt_{21} and Pt_{23} clusters

The lowest energy structures prefer the cubic pattern for Pt_{21} and Pt_{23} clusters. (*21a*) can be obtained from (*18c*) by capping three atoms on a square face. (*23a*) is obtained by adding a square pyramidal Pt_5 unit on a square face of (*18c*). Relative to (*21a*), a six-fold trilayer (*21b*) which is the most stable structure by using empirical method [27] lies 0.19 eV higher in energy. A COB (*21c*), a LT isomer (*21d*) and a $D_{6\,h}$ isomer (*21e*) are 0.354, 1.082 and 1.644 eV higher in energy, respectively. For Pt_{23}, a bell-shaped structure (*23b*) with C_{2v} symmetry lies 0.226 eV higher in energy. Analogously with (*23a*), (*23c*) can be viewed as a square pyramidal Pt_5 unit on a square face of a Pt_{18} triangular prism. However, it lies significantly higher in energy (0.258 eV) than (*23a*). A COB isomer (*23d*) obtained by adding four atoms on a center octahedron is exceedingly higher in energy (0.884 eV). Previously reported centered decahedron [25] and truncated decahedral isomer [27] are 0.583 and 1.181 eV higher than (*23a*).

3.1.4. Pt_{22} cluster

For Pt_{22}, the most stable isomer (*22a*, triplet) is a C_s structure. Three different spin multiplicities (M = 1, 3 and 5) have been examined for Pt_n (n = 15–24) clusters. However, it is found that only the most stable Pt_{22} cluster is in triplet and other sized clusters in singlet. A notable result is its magnetic properties, and the magnetic moment is 2 μB. There are large variations in the local magnetic moment on different sites ranging from 0.026 to 0.346 μB/atom. The COB isomer (*22b*) with C_{3v} symmetry adopts 19-atom centered octahedron framework and adds three atoms in three three-fold symmetric sites. It is only 0.086 eV higher in energy than the most stable structure. (*22c*) and (*22d*) obtained by capping a four-atom layer on a square face of (*18c*) and (*18a*), lie significantly higher in energy (0.311, 0.373 eV) than (*22a*). An empty center decahedral cage regarded as the lowest energy structure in Ref. [25] is also 0.618 eV higher in energy. The face-sharing icosahedral isomers obtained by Ref. [27] using empirical potentials lie 1.507 eV higher in energy than the present (*22a*).

3.2. General remarks for the structural motifs

From the above discussion, the medium-sized Pt_n (n = 15–24) clusters are not fond of closed-packed structures (i.e. icosahedron, decahedron-based) with higher compactness or average coordination number (ACN) as shown in Table 2. The bent rhombic dodecahedron based (DODB) configurations dominate the Pt_n (n = 16, 19, 24) motif; Pt_n (n = 17–18, 20) clusters favor the layered triangular (LT) pattern; Pt_{21} and Pt_{23} clusters prefer the cubic pattern, and Pt_{22} is a C_s symmetric structure. Binding energy per atom as a function of cluster size for the different growth pattern isomer demonstrates the structural evolution. Fierce competition among the four motifs is found in Fig. 2. As a whole, the open shell structures are favorable for the medium-sized platinum clusters. The COB motif which is a fragment of bulk platinum solids doesn't play a dominant role in the medium-sized platinum clusters.

4. Electronic properties of the lowest-energy Pt_n (n = 15–24) clusters

Ionization potentials (IPs), electron affinities (EAs) and HOMO–LUMO gaps are fundamental quantities of great importance in

many areas of chemistry and physics. HOMO–LUMO gaps, vertical ionization potentials (IPs) as a function of the lowest-energy Pt_n (n = 15–24) clusters are plotted in Fig. 3.

In Fig. 3, the values of vertical IPs of Pt_n have a small fluctuation and range from 6.22 to 6.72 eV, while the HOMO–LUMO gaps have a broad range from 0.03 to 1.2 eV. Compared the two lines, the HOMO–LUMO gaps, vertical ionization potentials (IPs) variety trends are basically similar. Pt_{15} has an extraordinarily large HOMO–LUMO gap (1.203 eV) and vertical IP (6.724 eV). As a continuation of the Pt_{15} cluster with an extremely high stability, a large gap and IP value for Pt_{16} are also found. In addition, Pt_{19} and Pt_{24} clusters belonging to DODB growth pattern have relatively larger gaps comparing to neighbor-size clusters. The local maxima of IPs at Pt_{23} and gaps at Pt_{21} are also observed. The Pt_{15} cluster is identified as a "magic" numbered cluster.

To further discuss the correspondence between the electronic and geometry structures of these platinum clusters, the partial density of states (PDOS) of Pt_n clusters are computed and shown in Fig. 4. In all the cases studied, hybridization of sp and d electrons can be observed. The PDOS profiles tend to be shifted to the lower energy with the size increasing. Careful examinations show that PDOS exhibit distinct features for platinum clusters belonging to different structural pattern. The Pt_{15} cluster has more well-defined peaks comparing with other isomers. This is probably due to a higher O_h geometrical symmetry. The partial density of states crossing the Fermi level has high value, and the d electron PDOS is divided into two spiculate peaks around the Fermi level. Two characteristics of DODB growth pattern are found. The first is that the d electron band has four main peaks at Pt_n (n = 15–16, 19 and 24) clusters compared with other motifs; the second is that DODB configurations possess relatively broad d-bandwidth. For Pt_{17}, Pt_{18} and Pt_{20} clusters, their common features are as follows: firstly, two d distinct peaks have almost coequal power to dominate the electronic properties although one of d distinct peaks is also divided into two little peaks at Pt_{18}; secondly, they have narrow d electron bandwidth. The d electron PDOS of Pt_{22} seems to have only two distinct peaks and no keen-edged peaks.

5. Conclusions

An unbiased search for the global minimum structures and structural evolution of Pt_n (n = 15–24) clusters have been conducted using a combination of empirical GA simulation and first-principles spin-polarized DFT method. Four kinds of structural motifs: bent rhombic dodecahedron based (DODB), layered triangular (LT), cuboctahedron based (COB) and cubic patterns are obtained. As a whole, the most stable isomers prefer the open structural motifs other than atomic closed shell structures. The DODB structures dominate the motif of medium-sized Pt_n (n = 15–16, 19 and 24) clusters. The DODB motif can be related to the extraordinary stability of the Pt_{15}, which is also demonstrated by the higher HOMO–LUMO gap and vertical ionization potential. The Pt_n (n = 17–18, 20) prefer LT pattern, while Pt_n (n = 21, 23) clusters lean to cubic mode. Pt_{22} is a C_s structure. Pt_n clusters at n = 15, 18 and 24 are relatively more stable and called as "magic" numbered. We also examined three different spin multiplicities (M = 1, 3 and 5) and found the most stable structure of Pt_{22} cluster is the only one in triplet not in singlet state. The HOMO–LUMO gaps, vertical ionization potentials (IPs) of Pt_n (n = 15–24) clusters have been calculated. The PDOS results show that different motifs have different features and may provide useful information for experiments.

Acknowledgement

This project was supported by Science Research Foundation of Dalian University of Technology (No. 842205).

References

[1] K.J. Klabunde, Nanoscale Materials in Chemistry, Wiley, New York, 2001.
[2] (a) G.V. Smith, S. Tjandra, M. Musoiu, T. Wiltowski, F. Notheisz, M. Bartók, I. Hannus, D. Ostgard, V. Malhotra, J. Catal. 161 (1996) 441;
(b) J.M. Wei, E. Iglesia, J. Phys. Chem. B 108 (2004) 4094.
[3] G.W. Crabtree, M.S. Dresselhaus, M.V. Buchanan, Phys. Today 57 (2004) 39.
[4] M.B. Airola, M.D. Morse, J. Chem. Phys. 116 (2002) 1313.
[5] J.C. Fabbi, J.D. Langenberg, Q.D. Costello, M.D. Morse, L. Karlsson, J. Chem. Phys. 115 (2001) 7543.
[6] S.K. Gupta, B.M. Nappi, K.A. Gingerich, Inorg. Chem. 20 (1981) 966.
[7] K. Jansson, R. Scullman, J. Mol. Spectrosc. 61 (1976) 299.
[8] S. Taylor, G.W. Lemire, Y.M. Hamrick, Z. Fu, M.D. Morse, J. Chem. Phys. 89 (1988) 5517.
[9] (a) J. Ho, M.L. Polak, K.M. Ervin, W.C. Lineberger, J. Chem. Phys. 99 (1993) 8542;
(b) K.M. Ervin, J. Ho, W.C. Lineberger, J. Chem. Phys. 89 (1988) 4514;
(c) A. Grushow, K.M. Ervin, JACS 117 (1995) 11612.
[10] N. Pontius, P.S. Bechthold, M. Neeb, W. Eberhardt, J. Electron. Spectrosc. Relat. Phenom. 106 (2000) 107.
[11] C.M. Chang, M.Y. Chou, Phys. Rev. Lett. 93 (2004) 133401.
[12] E. Aprà, A. Fortunelli, J. Phys. Chem. A 107 (2003) 2934.
[13] W.Q. Tian, M.F. Ge, B.R. Sahu, D.X.WangT. Yamada, S. Mashiko, J. Phys. Chem. A 108 (2004) 3806.
[14] S.H. Yang, D.A. Drabold, J.B. Adams, P. OrdejÓn, K. Glassford, J. Phys.: Condens. Matter 9 (1997) 39.
[15] E. Aprà, A. Fortunelli, J. Mol. Struct.: Theochem 501 (2000) 251.
[16] N. Watari, S. Ohnishi, Phys. Rev. B 58 (1998) 1665.
[17] R.C. Longo, L.J. Gallego, Phys. Rev. B 74 (2006) 193409.
[18] L.L. Wang, D.D. Johnson, Phys. Rev. B 75 (2007) 235405.
[19] K. Bhattacharyya, C. Majumder, Chem. Phys. Lett. 446 (2007) 374.
[20] L. Xiao, C.W. Li, J. Phys. Chem. A 108 (2004) 8605.
[21] A.H. Nie, J.P. Wu, C.G. Zhou, S.J. Yao, L. Chen, R.C. Forrey, H.S. Cheng, Int. J. Quantum Chem. 107 (2007) 219.
[22] A. Fortunelli, J. Mol. Struct.: Theochem 493 (1999) 233.
[23] M.N. Huda, M.K. Niranjian, B.R. Sahu, L. Kleinman, Phys. Rev. A 73 (2006) 053201.
[24] S. Varga, B. Fricke, H. Nakamatsu, T. Mukoyama, J. Anton, D. Geschke, A. Heitmann, E. Engel, T. Baştuğ, J. Chem. Phys. 112 (2000) 3499.
[25] V. Kumar, Y. Kawazoe, Phys. Rev. B 77 (2008) 205418.
[26] J. Uppenbrink, D.J. Wales, J. Chem. Phys. 96 (1992) 8520.
[27] Jonathan P.K. Doye, D.J. Wales, New J. Chem. 22 (1998) 733.
[28] A. Sebetci, Ziya B. Güvenç, Surf. Sci. 525 (2003) 66.
[29] A. Sebetci, Z.B. Güvenç, Eur. Phys. J. D 30 (2004) 71.
[30] A. Sachdev, R.I. Masel, J.B. Adams, Catal. Lett. 15 (1992) 57.
[31] A. Sachdev, R.I. Masel, J.B. Adams, Z. Phys. D 26 (1993) 310.
[32] D.M. Deaven, K.M. Ho, Phys. Rev. Lett. 75 (1995) 288.
[33] M.A. Karolewski, Radiat. Eff. Defect Solids 153 (2001) 239.
[34] F. Cleri, V. Rosato, Phys. Rev. B 48 (1993) 22.
[35] V. Rosato, Philos. Mag. A 59 (1989) 321.
[36] A.P. Sutton, J. Chem, Philos. Mag. Lett. 61 (1990) 139.
[37] J. Wang, G. Wang, J. Zhao, Phys. Rev. B 66 (2002) 035418.
[38] J.P. Perdew, K. Burke, M. Ernzerhof, Phys. Rev. Lett. 77 (1996) 3865.
[39] B. Delly, Phys. Rev. B 66 (2002) 155125.
[40] B. Delly, J. Chem. Phys. 92 (1990) 508.